Correlation of hepatic fractional extracellular space using gadolinium enhanced MRI with liver stiffness using magnetic resonance elastography

Michael L. Wells,[1] Michael R. Moynagh,[1] Rickey E. Carter,[2] Robert A. Childs,[1] Cameron E. Leitch,[1] Joel G. Fletcher,[1] Benjamin M. Yeh,[3] Sudhakar K. Venkatesh[1]

[1]Department of Radiology, College of Medicine, Mayo Clinic, 200 First St. SW, Rochester, MN 55905, USA
[2]Department of Health Sciences Research, Mayo Clinic, Rochester, MN, USA
[3]Department of Radiology, University of California San Francisco, San Francisco, CA, USA

Abstract

Purpose: To compare MR hepatic fractional extracellular space (fECS) to liver stiffness (LS) with magnetic resonance elastography (MRE) for evaluation of liver fibrosis.
Methods and materials: 71 consecutive patients with suspected chronic liver disease underwent standard liver MRI with MR elastography and additional delayed Gd-DTPA-enhanced sequences at 5 and 10 min in order to calculate hepatic fECS (%) and LS (kilopascals, kPa). Two radiologists blinded to clinical history examined MR images and calculated fECS and LS in identical locations for every patient. Interobserver agreement was calculated using the intraclass correlation coefficient. Pearson's correlation was calculated for LS and fECS measures, as was the area under the receiver operatic curve (AUROC), sensitivity and specificity of fECS to predict liver stiffness ≥ 2.93 and ≥ 5 kPa. The sensitivity of fECS for detecting fibrosis was separately analyzed in the subgroup of patients without anatomic findings of cirrhosis.
Results: Substantial to excellent interobserver agreement for both LS and fECS measurements was seen with intraclass correlation of 0.88 (95% CI 0.81–0.92) for LS, 0.77 (95% CI 0.66–0.85) for $fECS_5$ and 0.76 (95% CI 0.64–0.84) for $fECS_{10}$. A significant correlation was found between MRE and $fECS_5$ ($r = 0.47$, $p < 0.0001$) and $fECS_{10}$ ($r = 0.44$, $p < 0.0001$). The performance of fECS improved for detection of advanced fibrosis (≥ 5 kPa) with AUROC, sensitivity and specificity of 0.72, 38%, and 94% for $fECS_5$ and 0.72, 67%, and 66% for $fECS_{10}$.
Conclusion: fECS correlates modestly with MRE-determined LS. fECS at MRI is a simple calculation to perform and may represent a practical way to suggest the presence of fibrosis during routine liver evaluation.

Key words: MRI—Fractional extracellular space—Hepatic fibrosis—Hepatic extracellular space—Gadolinium—MR elastography—Liver stiffness—Liver fibrosis

Correspondence to: Sudhakar K. Venkatesh; *email:* Venkatesh.Sudhakar@mayo.edu

Chronic liver disease resulting in hepatic fibrosis and cirrhosis is a leading cause of worldwide disability and death [1]. The most common etiologies of liver fibrosis worldwide include alcohol abuse, viral infections with hepatitis B and C, and nonalcoholic fatty liver disease (NAFLD) which has become a common source of liver disease in developed countries [1]. Chronic liver diseases, such as NAFLD, are expected to become increasingly prevalent in the upcoming decades; correspondingly, the need for cost effective and accessible methods of evaluation will also increase.

Chronic liver disease results in progressive accumulation of interstitial fibrosis. Accurate staging is important to predict complications, which increase with degree of liver fibrosis, and to monitor response to therapy as fibrosis can be at least partially reversed at all stages, including cirrhosis [2–4]. Percutaneous biopsy is currently considered the reference standard for the diagnosis

of cirrhosis and to stage liver fibrosis. The limitations of biopsy include interobserver variability, sampling error, high cost, limited patient acceptance, and complications such as pain and hemorrhage [3, 5, 6]. These factors render biopsy inadequate for routine patient screening and serial evaluation of disease progression or response to treatment.

Noninvasive tests represent a potential cost effective alternative to biopsy for the detection and staging of liver fibrosis, and include several imaging methods. Conventional anatomic findings of cirrhosis (e.g., surface nodularity, parenchymal atrophy, etc.) have been shown to have low performance at US, CT, and MRI for the assessment of fibrosis and are insufficient for guiding patient management [7–9]. Dynamic enhancement techniques such as arterial enhancement fraction calculation have shown modest accuracy in predicting hepatic fibrosis [10, 11]. Ultrasound- and MRI-based methods which interrogate tissue stiffness in the form of elastography have demonstrated the best results for hepatic fibrosis detection and staging [8, 12, 13]. MR elastography is currently the most accurate noninvasive technique available for estimating hepatic fibrosis [12, 14–16].

Evaluation of liver fibrosis has been performed using CT estimates of the hepatic fractional extracellular space (fECS) [17–20]. The liver can be represented as a three-compartment model comprises the intravascular space, intracellular space, and extracellular space. Given time for equilibration, an extracellular contrast agent will diffuse through tissue to reach roughly equal concentrations within the intravascular and extracellular spaces of the liver. Fibrosis in liver is associated with increased extracellular space surrounding the collagen fibers; therefore, fECS in fibrotic regions will be higher than normal liver parenchyma. fECS calculated from attenuation measurements taken from noncontrast and 10-min delayed phase images have been shown to correlate well with patient MELD score and predictive of cirrhosis [18].

MRI-based calculation of extracellular space for estimation of myocardial fibrosis has been performed and validated [21, 22]. MRI-based calculation of the hepatic interstitial volume has also been used for the study of liver amyloid deposition [23]. The T1 mapping technique used for estimation of T_1 values these prior studies is time consuming and not practical for routine clinical use. Simple signal intensity measurements, without T_1 mapping correction, taken at routine clinical MRI could be easily employed at routine liver evaluation with little additional scan time, no additional equipment, and minimal radiologist effort. To our knowledge this has not been previously studied. If reliable, the measurement of MRI fECS would be an easily obtainable estimation of hepatic fibrosis for use in routine clinical liver MRI. The purpose of this study was to test the hypothesis that a simple MRI-based calculation of fractional extracellular space correlates with a reference standard of liver stiffness (LS) measured using MR elastography.

Methods

Patients

The study was conducted with a retrospective, observational design. The study was HIPAA compliant and need for informed consent was waived by our institutional review board. Between the dates of January 1 2013 to April 8 2013, 71 consecutive patients with suspected chronic liver disease of any etiology undergoing contrast-enhanced MRI with MRE as part of routine clinical evaluation were included in the study. Patients were assessed for adequate renal function with the estimated glomerular filtration rate per our institution's routine guidelines prior to IV contrast administration. Limited chart review was performed with recording of patient age, sex, and clinically diagnosed etiology of liver disease and hematocrit (HCT).

Imaging

All imaging was performed on a clinical 1.5T MRI system (Signa, GE Healthcare, Waukesha, WI) using a phased array torso coil.

MRE

Elastography was performed using a 19 × 15 cm passive driver secured with an elastic band over the liver. An active acoustic generator was used and transmitted 60 Hz vibrations to the passive drive by a 25-foot long vinyl tube. Shear waves within the liver were imaged using a 2-dimensional gradient echo-based MRE phase contrast sequence with the following parameters; TR/TE = 100/23.6 ms, bandwidth = ±31.25 kHz, flip angle = 30, FOV = 32–42 cm, matrix 256 × 92, slice thickness = 10 mm, gap = 5 mm. Four slices through the widest axial portion of the liver were acquired in each patient. Each slice was acquired with 12–16 s breath holds at end expiration. The wave images were automatically processed by an inversion algorithm to produce a stiffness map in units of kilopascals (kPa).

MRI

Standard imaging protocol included pre- and postcontrast-enhanced fat-suppressed T1-weighted liver acquisition with volumetric acceleration (LAVA) performed in the axial plane with 4 mm slice thickness. Postcontrast imaging was performed with three-phase dynamic acquisition (i.e., arterial, portal, and hepatic phases), and a 5- and a 10-min equilibrium-phase acquisition. Other sequences obtained included axial T2-weighted fat-suppressed fast spin echo, diffusion weighted imaging, in and opposed phase T1-weighted images, coronal T2-weighted single-shot fast spin echo. Gd-DTPA-BMA Gadodiamide (Omniscan, GE Healthcare) intravenous

contrast was injected at routine clinical dosing of 0.01 mmol/Kg injected at a rate of 2–3 mL/s followed by a 30-mL saline flush. Gd-DTPA-BMA distributes into the vascular and extracellular interstitial spaces without intracellular accumulation [24].

Image analysis

Two readers, including an abdominal fellowship trained radiology staff with 15 years of experience and an abdominal imaging radiology fellow, reviewed all imaging independently. A DICOM workstation (Advantage Workstation, GE Healthcare, Waukesha, WI) was used for image review which was performed over a 3-week period. Readers were blinded to all patient clinical information.

LS and fECS calculation

The calculations were performed on an Advantage Windows station (AW2.0, GE Healthcare, Waukesha, WI). LS was manually measured from the MRE stiffness map using oval-shaped region of interest (ROI) (Fig. 1). A single ROI was placed on the liver on a single MRE slice in each subject and made as large as possible (>100 mm^2), while avoiding the liver capsule, fissures, regions of wave interference, vessels larger than 3 mm, masses, and regions of low statistical confidence [13]. LS values were translated into estimated fibrosis stages based on a reference scale, as previously reported in the literature [16]. For fECS measurements, readers measured the signal intensity of the aorta and liver on nonenhanced and both 5- and 10-min delayed enhanced images for each patient. Additionally, the liver ROI's on the MRE stiffness maps were mapped onto the corresponding locations on the precontrast and postcontrast images so that these measurements would be made in the same location. fECS was calculated based on the formula: $\%fECS = (\text{Liver}_{enh} \div \text{Liver}_{nonenh}) / (\text{Aorta}_{enh} \div \text{Aorta}_{nonenh}) \times (1 - HCT)$. Reader-specific estimates of fECS were obtained using the individual measurements obtained by each reader. The measurement of fECS and stiffness made by the more experienced reader were used for calculations of fECS performance. The measurements of fECS and stiffness made by the less experienced reader were used for calculation of interobserver variability.

Visual assessment of imaging findings of chronic liver disease

Anatomic imaging was also reviewed for evidence of cirrhosis according to the following five criteria: (1) morphologic changes of cirrhosis (nodular liver border, right lobar atrophy, caudate-right lobe ratio, widened fissures, right posterior hepatic notch), (2) visible bridging fibrosis, (3) regenerative nodules, (4) ascites, and (5) other findings of portal hypertension (splenomegaly, portosystemic shunts) (Fig. 2). Each of the five criteria was graded on a 3-point scale 0–2, with 0 being absent, 1 equivocal finding, and 2 present. The scores of the five criteria were summed with total score >2 defined as obvious chronic liver disease.

Statistics

Interobserver agreement was visually examined using Bland–Altman plots. A quantitative analysis of interobserver agreement was conducted using the intraclass correlation coefficient (ICC) derived from a one-way random effects model. The ICC values were interpreted against the Landis and Koch thresholds for kappa (i.e., <0.20 slight agreement; 0.21–0.40 fair agreement, 0.41–0.60 moderate agreement, 0.61–0.80 substantial agreement, and 0.81–1.00 excellent agreement) [25].

The association of LS and fECS was assessed with the Pearson's correlation test. In addition, a regression spline (restricted cubic B-spline) was fitted allowing second-degree polynomials and three equally spaced 'knots' (points of inflection) to better estimate a functional form between fECS and MRE. Area under the ROC curve was used to quantify the ability of fECS to discriminate fibrotic from nonfibrotic tissue. At least stage 1 fibrosis (≥ 2.93 kPa as determined by MRE) and at least stage 4 fibrosis (≥ 5.0 kPa as determined by MRE) were separately modeled as "fibrotic". For each of the stiffness definitions, Youden's index was used to determine fECS threshold values to classify livers based on fECS. Area under the receiver operating curve (AUROC), sensitivity, specificity, and 95% confidence intervals were calculated for each fibrosis threshold at each fECS delay (5 and 10 min). To assess for ability of fECS and to detect fibrosis in the absence of anatomic change, the optimal fECS thresholds were compared with the subsets of patients without definite anatomic findings of cirrhosis. Statistical analysis was conducted using the SAS System version 9.3 (Cary, NC).

Results

Patients

71 patients (27 female, 44 male) were enrolled in the study. Mean patient age was 52 years (range 18–84). Chronic liver disease etiology included primary sclerosing cholangitis (21), hepatitis C (11), alcoholic liver disease (9), nonalcoholic fatty liver disease (7), nonalcoholic steatohepatitis (7), primary biliary cirrhosis (4), autoimmune hepatitis (3), congestive hepatopathy (3), chronic acetaminophen or methotrexate use (3), alpha 1 antitrypsin deficiency (2), hepatitis B (2), schistosomiasis (1), Wilsons disease (1), elevated liver function tests (1); 4 patients were diagnosed with multiple conditions
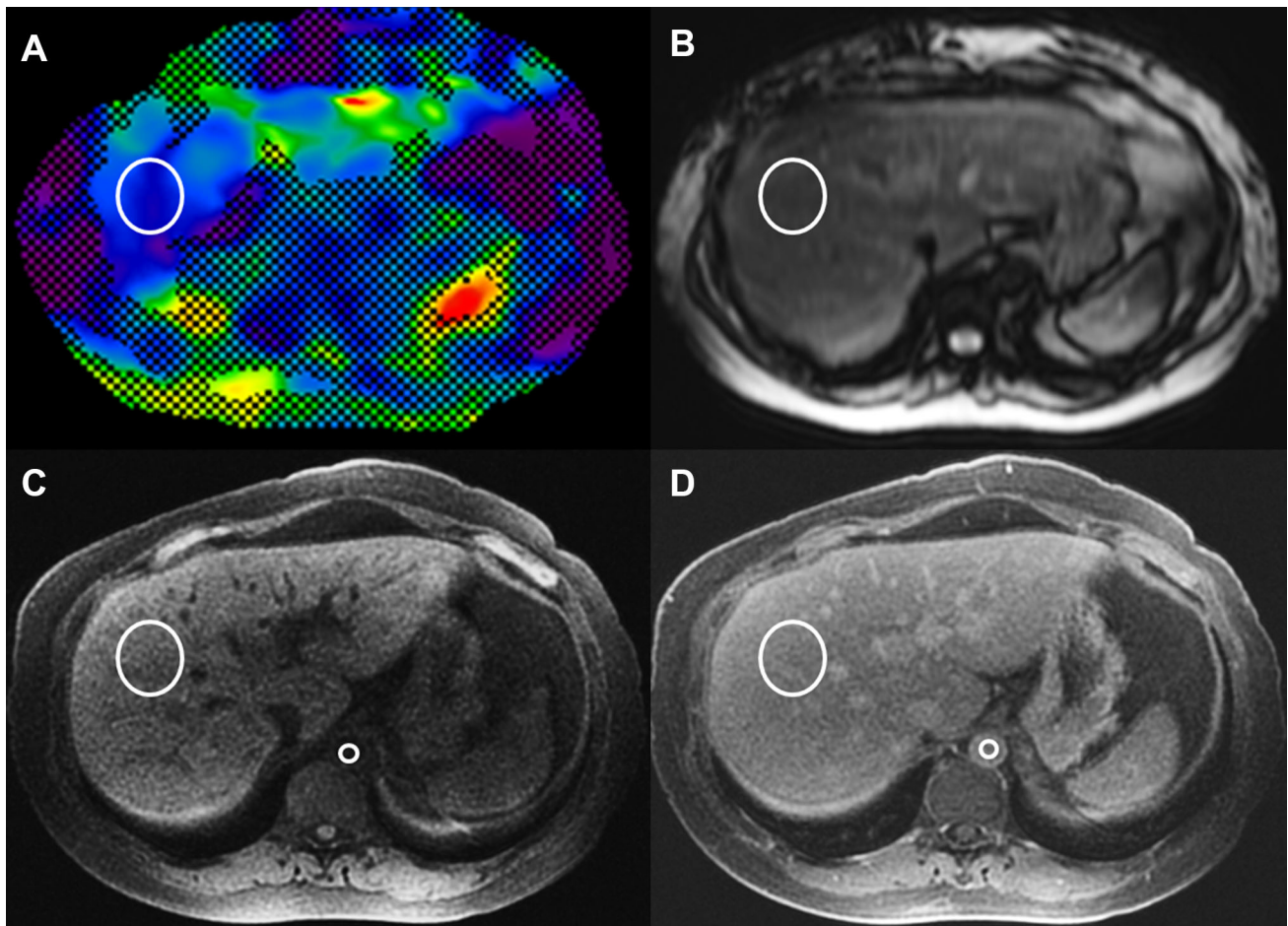
Fig. 1. Measurement of liver stiffness and fECS. **A** ROI was placed on the elastogram to avoid regions of wave interference, large vessels masses, and fissures. **B** The ROI from the elastogram was mapped onto the elastography magnitude image which served as an anatomic reference. **C**, **D** The elastogram ROI was then mapped onto the precontrast (**C**) and postcontrast (**D**) axial fat-saturated T1-weighted images. Additional ROIs were drawn on the aorta of the same precontrast and postcontrast MRI images.

affecting the liver. HCT was obtained on an average of 12.4 days within the MRI scan.

Imaging

Measured LS values had an average of 4.84 kPa (median 3.8 kPa, range 1.30–20.83). 5-min fECS ($fECS_5$) values had an average of 24.0% ± 6% (median 24.0%, range 9.0%–37.9%). 10-minute fECS ($fECS_{10}$) values had an average of 27.2% ± 6% (median 26.8%, range 12.5%–43.5%). fECS increased significantly by 3.5% (95% CI 3.5%–4.8%; $p < 0.0001$) between 5 and 10 min. Reader agreement was substantial to excellent for both LS measurement and fECS values with intraclass correlation of 0.88 (95% CI 0.81–0.92) for MRE stiffness, 0.77 (95% CI 0.66–0.85) for $fECS_5$, and 0.76 (95% CI 0.64–0.84) for $fECS_{10}$. Scoring of anatomic findings revealed 17 patients with obvious findings of liver fibrosis and 54 patients without obvious findings; with an average visual anatomic score for finding of chronic liver disease being 1.27 (range 0–6).

A statistically significant correlation was found between fECS and LS. Pearson correlation coefficient was 0.47 ($p < 0.0001$) and 0.44 ($p < 0.0001$) for $fECS_5$ and $fECS_{10}$, respectively. Figure 3 shows the results of the splined fit of MRE regressed on $fECS_{10}$. 49% of the variation in LS was explained by the fitted spline and the relationship had a statistically significant correlation ($p = 0.0001$).

The optimal threshold values obtained by Youden's Index for $fECS_5$ were ≥0.28 for LS ≥2.93 kPa and ≥0.30 for LS ≥5 kPa and for $fECS_{10}$ were ≥0.28 for LS LS ≥2.93 kPa and ≥0.27 for LS ≥5 kPa.

Table 1 demonstrates the estimated performance of MR $fECS_5$ and $fECS_{10}$ for prediction of Stage 1 and Stage 4 fibrosis using the threshold calculated. AUROC for $fECS_5$ was 0.59 and 0.72 for stage 1 and 4 fibrosis, respectively. AUROC for $fECS_{10}$ was 0.53 and 0.72 for
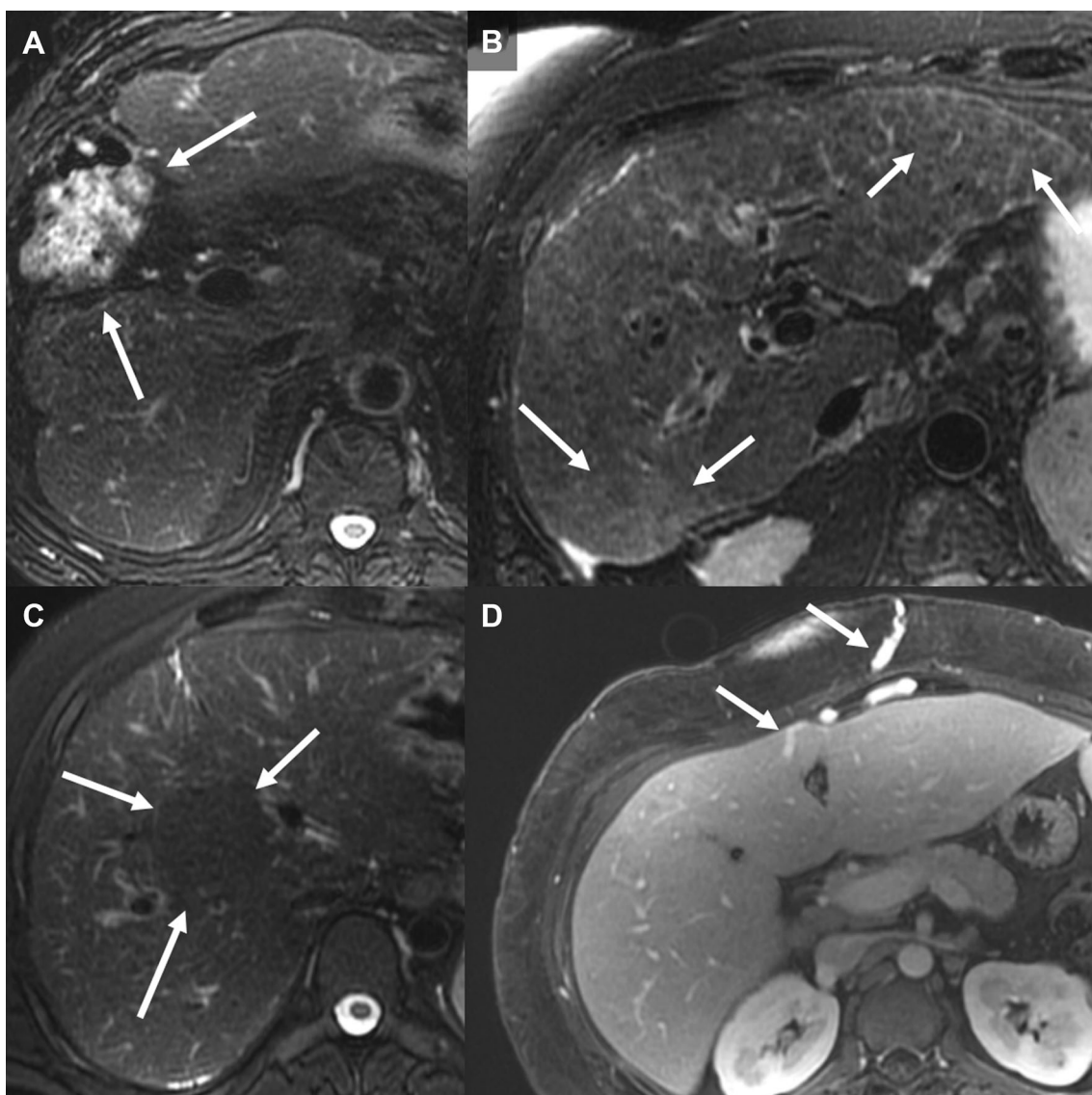
Fig. 2. Examples of anatomic findings of cirrhosis. **A** Patient with nodular cirrhotic liver due to alcoholism and markedly widened gallbladder fossa containing the hepatic flexure of the colon (*arrows*). **B** Another patient with nonalcoholic steatohepatitis induced cirrhosis with nodular liver, T2 hyperintense bridging fibrosis (*arrows*) and splenomegaly (not shown). **C** Patient with nonalcoholic steatohepatitis-induced cirrhosis with large regenerative nodule (*arrows*). **D** Patient with primary biliary cirrhosis and portosystemic shunt (*arrows*).

stage 1 and 4 fibrosis, respectively. This analysis shows that for the detection of Stage 1 fibrosis, $fECS_{10}$ is more sensitive than $fECS_5$, with sensitivity increasing from 28% (95% CI 17%–43%) to 44% (95% CI 30%–58%), but does so at the expense of specificity. $fECS_{10}$ was also more sensitive than $fECS_5$, for detecting stage 4 fibrosis [sensitivity of 38% (95% CI 21%–57%) and 67% (95% CI 47%–82%), for $fECS_5$ and $fECS_{10}$ respectively].

Of the 71 patients in the study cohort, 17 patients had definite imaging findings of chronic liver disease based on the previously described visual score. In the subgroup of 54 patients without definite morphologic findings of cirrhosis, 48% (26/54) had MRE stiffness values of 2.93 kPa or higher, indicating at least Stage 1 fibrosis. Using the $fECS_{10\ min}$ threshold of ≥28% for Stage 1 and higher fibrosis, $fECS_{10}$ would have identified 42% (11/26) of patients in this group. In the group of patients without definite morphologic findings of cirrhosis 13% (7/54) had LS ≥5 kPa indicating stage 4 fibrosis. $fECS_{10\ min}$ using a threshold of ≥28% would have detected 57% (4/7) of these patients. In the group of patients with LS <2.93 kPa (28/71), indicating normal liver stiffness, the $fECS_{10\ min}$ value was <28% in 75% (21/28).

Discussion

Our study showed that a simple calculation of fECS performed at MRI has high interobserver agreement and correlates modestly with LS measured at MRE. The performance of calculated fECS improved with prediction of advanced fibrosis using the higher fECS cutoff values. The significant correlation between fECS and LS with MRE suggests that fECS may have potential role in the diagnosis and monitoring of patients with chronic liver disease. This is particularly important given the increasing prevalence of chronic liver disease and the need for cost effective methods of screening and monitoring. The performance of MR fECS in our study does not suggest that it would be a replacement for noninvasive assessments of fibrosis such as MRE or ultrasound-based elastography. However, fECS may be useful at institutions in which these alternative techniques are not available or for patients already undergoing MRI. The added information is complementary to other quantitative MRI assessments of chronic liver disease such as

Fig. 3. Regression plot demonstrating correlation between fECS measured at 10 min and MRE stiffness.

those for hepatic steatosis and can be obtained without the radiation dose penalty imposed by CT.

The performance of fECS at MRI in our study was modest. When compared with CT measures of fECS, the performance was not as strong as that reported by Zissen et al. but was similar when compared with two subsequent reports [18–20]. There are several factors which may influence the accuracy of fECS measurement at MRI when compared with CT. One difficulty is obtaining accurate estimates of gadolinium concentration at MRI based on signal intensities. While measured attenuation at CT is directly proportional to iodinated contrast concentration, signal intensity of the liver at MRI is not directly proportional to gadolinium concentration and depends on many confounding factors [26, 27]. Without appropriate scaling factors and references of known gadolinium concentration, only an estimate of relative concentrations can be obtained by measuring absolute signal intensities at MRI. Gadolinium concentration is directly proportional to $1/T_1$ and T_1 estimation can be obtained by employing mapping techniques which require obtaining additional sequences and performing additional calculations [21–23, 27]. While estimation of fECS using T1 mapping techniques may improve the performance of MRI for detection of fibrosis, the techniques currently available are not practical for routine clinical use.

Another factor which may influence MRI fECS when compared with CT is the difference in volume of injected contrast media. It has been shown that increased volume of contrast injection leads to improved delayed phase image quality when assessing fibrosis; the small contrast bolus at MRI relative to CT may lead to decreased contrast to noise ratio in the delayed phase [28]. Perfusion of the liver decreases in the setting of cirrhosis and decreased flow to an organ of interest delays the distribution of contrast to an equilibrium state [29, 30]. This could potentially exacerbate both the effect of small bolus volume on uniform extracellular distribution and the optimal timing of delay phase imaging leading to less
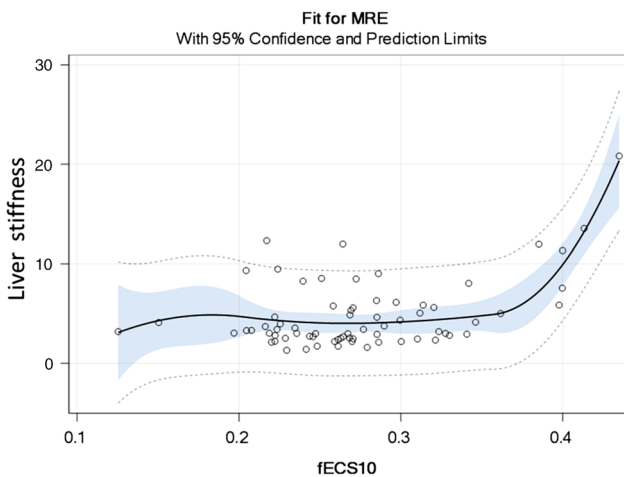
Table 1. Accuracy, sensitivity, and specificity of fECS for predicting fibrosis

	Threshold for positivity	Metric	Estimate, % (n/N)	95% CI
fECS$_{5 min}$	≥Stage 1 fibrosis (MRE ≥ 2.93 kPa) threshold: ≥0.28	Accuracy	57 (36/71)	39–62
		Sensitivity	28 (13/46)	17–43
		Specificity	92 (23/25)	75–98
	Stage 4 fibrosis (MRE ≥ 5.0 kPa) threshold: ≥0.30	Accuracy	75 (53/71)	63–83
		Sensitivity	38 (9/24)	21–57
		Specificity	94 (44/47)	82–98
fECS$_{10 min}$	≥Stage 1 fibrosis (MRE ≥ 2.93 kPa) threshold: ≥0.28	Accuracy	72 (18/25)	52–86
		Sensitivity	44 (20/46)	30–58
		Specificity	72 (18/25)	52–86
	Stage 4 fibrosis (MRE ≥ 5.0 kPa) threshold: ≥0.27	Accuracy	66 (47/71)	55–76
		Sensitivity	67 (16/24)	47–82
		Specificity	66 (31/47)	52–78

Measures of diagnostic accuracy are determined for threshold values that were obtained by maximizing Youden's index for stiffness ≥2.93 and ≥5 kPa for both fECS at 5 and 10 min
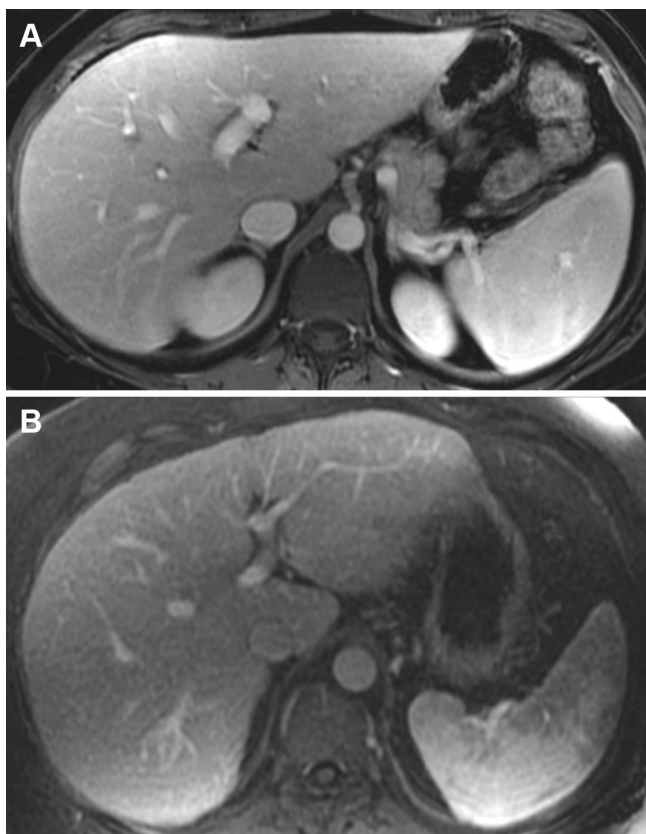
Fig. 4. Two patients without anatomic findings of cirrhosis in which fECS could have suggested significant fibrosis or cirrhosis. **A** Patient with primarily biliary cirrhosis and autoimmune hepatitis had an average $fECS_{10}$ of 31% and MRE stiffness value of 5.2 kPa. **B** Patient with nonalcoholic steatohepatitis and hepatitic C had an average $fECS_{10}$ of 39% and MRE stiffness of 5.3 kPa.

consistent results. Continuous infusion techniques have been used to ensure that delayed phase imaging is performed during equilibrium distribution of contrast material [23]. However, the use of continuous infusion not practical for routine clinical use and prior studies performed in CT have shown efficacy of bolus techniques for identifying fibrosis when using as little as a 120 s delay [20].

The regional distribution of scar deposition in hepatic fibrosis is known to vary widely within the liver. MRI fECS has the potential to sample the entire liver volume. This represents a potential major benefit over techniques such as liver biopsy which samples a very small portion of the liver or elastography methods such as 2D GRE MRE which typically samples four 10 mm thick slices of the liver or ultrasound elastography which has limited tissue penetration and sampling. This study did not compare measurements taken from multiple locations within individual livers but multiple regions of interest could easily be used. Future study would be useful to assess the ability of fECS to detect regional variation of

fibrosis. The nonuniform accumulation of gadolinium in the delayed phase also facilitates the use of scoring systems based on parenchymal heterogeneity [31, 32]. These systems have shown correlation with degree of parenchymal fibrosis and could potentially be combined with fECS measurement to increase accuracy of fibrosis detection.

One difficulty in making the diagnosis of cirrhosis is the fact that the liver can appear anatomically normal despite the presence of advanced fibrosis. Anatomic findings are known to have poor performance, particularly for detection of early fibrosis [7, 9]. Our results demonstrate the ability of MRI fECS to suggest the presence of fibrosis in the absence of anatomic findings of cirrhosis or portal hypertension (Fig. 4). fECS has the potential to suggest the presence of fibrosis in many patients without diagnostic anatomic findings. The ability to detect these cases at routine MRI may represent a major clinical benefit of MRI fECS and may be particularly valuable in locations in which MRE is not available.

Several limitations of the study not discussed above are acknowledged. Our sample size was modest, and larger studies are required to establish the utility of fECS. Biopsy and histopathology would have been ideal to use as a gold standard reference, but was not practical to perform for purposes of our study which used examinations obtained for clinical purposes. MRE has a proven high diagnostic performance and can be reasonably viewed as an acceptable alternative to costly and invasive liver biopsy. Lack of liver biopsy does limit the study in that other potential causes of delayed contrast retention such as passive hepatic congestion or edema related to inflammation were not directly assessed. These conditions result in a potential expansion of the extracellular space and represent a confounding etiology for delayed phase gadolinium retention. Variable scar deposition and a relatively small ROI could have resulted in nonuniform stiffness calculations in our study due to sampling variability. This was likely minimized by the study design which entailed spatial correlation of fECS both and MRE measurement. While we would expect extracellular contrast agents to behave similarly, it is possible that use of an extracellular IV contrast agent other than gadodiamide could have led to different results. This could be assessed with a future study.

Conclusion

There is a modest but significant correlation between hepatic fECS measured at MRI and LS. The additional information obtained by measuring fECS at MRI may represent a practical way to suggest the presence of fibrosis during routine liver evaluation. The additional diagnostic information requires no extra equipment, minimal radiologist effort, and minimal additional scan time if a delayed phase of 10 min is acquired.

Compliance with ethical standards

Conflict of interest   There is no conflict of interest.

Ethical approval   All procedures performed in studies involving human participants were in accordance with the ethical standards of the institutional and/or national research committee and with the 1964 Helsinki declaration and its later amendments or comparable ethical standards. The study was approved by our institutional review board.

Informed consent   The requirement for informed consent was waived by our Institutional IRB, due to the retrospective design of the study.

References

1. Lim YS, Kim WR (2008) The global impact of hepatic fibrosis and end-stage liver disease. Clin Liver Dis 12(4):733–746. doi:10.1016/j.cld.2008.07.007
2. Lee YA, Friedman SL (2014) Reversal, maintenance or progression: what happens to the liver after a virologic cure of hepatitis C? Antivir Res 107:23–30. doi:10.1016/j.antiviral.2014.03.012
3. Schuppan D, Afdhal NH (2008) Liver cirrhosis. Lancet 371(9615):838–851. doi:10.1016/S0140-6736(08)60383-9
4. Bedossa P (2015) Reversibility of hepatitis B virus cirrhosis after therapy: who and why? Liver Int 35(Suppl 1):78–81. doi:10.1111/liv.12710
5. Venkatesh SK, Yin M, Ehman RL (2013) Magnetic resonance elastography of liver: clinical applications. J Comput Assist Tomogr 37(6):887–896. doi:10.1097/RCT.0000000000000032
6. Rousselet MC, Michalak S, Dupre F, et al. (2005) Sources of variability in histological scoring of chronic viral hepatitis. Hepatology 41(2):257–264. doi:10.1002/hep.20535
7. Venkatesh SK, Yin M, Takahashi N, et al. (2015) Non-invasive detection of liver fibrosis: MR imaging features vs MR elastography. Abdom Imaging 40(4):766–775. doi:10.1007/s00261-015-0347-6
8. Bonekamp S, Kamel I, Solga S, Clark J (2009) Can imaging modalities diagnose and stage hepatic fibrosis and cirrhosis accurately? J Hepatol 50(1):17–35. doi:10.1016/j.jhep.2008.10.016
9. Rustogi R, Horowitz J, Harmath C, et al. (2012) Accuracy of MR elastography and anatomic MR imaging features in the diagnosis of severe hepatic fibrosis and cirrhosis. J Magn Reson Imaging 35(6):1356–1364. doi:10.1002/jmri.23585
10. Bonekamp D, Bonekamp S, Geiger B, Kamel IR (2012) An elevated arterial enhancement fraction is associated with clinical and imaging indices of liver fibrosis and cirrhosis. J Comput Assist Tomogr 36(6):681–689. doi:10.1097/RCT.0b013e3182702ee3
11. Ou HY, Bonekamp S, Bonekamp D, et al. (2013) MRI arterial enhancement fraction in hepatic fibrosis and cirrhosis. AJR Am J Roentgenol 201(4):W596–W602. doi:10.2214/AJR.12.10048
12. Singh S, Venkatesh SK, Wang Z, et al. (2015) Diagnostic performance of magnetic resonance elastography in staging liver fibrosis: a systematic review and meta-analysis of individual participant data. Clin Gastroenterol Hepatol 13(3):440–451. doi:10.1016/j.cgh.2014.09.046
13. Venkatesh SK, Yin M, Ehman RL (2013) Magnetic resonance elastography of liver: technique, analysis, and clinical applications. J Magn Reson Imaging 37(3):544–555. doi:10.1002/jmri.23731
14. Ichikawa S, Motosugi U, Morisaka H, et al. (2015) Comparison of the diagnostic accuracies of magnetic resonance elastography and transient elastography for hepatic fibrosis. Magn Reson Imaging 33(1):26–30. doi:10.1016/j.mri.2014.10.003
15. Dyvorne HA, Jajamovich GH, Bane O, et al. (2016) Prospective comparison of magnetic resonance imaging to transient elastography and serum markers for liver fibrosis detection. Liver Int 36(5):659–666. doi:10.1111/liv.13058
16. Venkatesh SK, Ehman RL (2014) Magnetic resonance elastography of liver. Magn Reson Imaging Clin N Am 22(3):433–446. doi:10.1016/j.mric.2014.05.001
17. Varenika V, Fu Y, Maher JJ, et al. (2013) Hepatic fibrosis: evaluation with semiquantitative contrast-enhanced CT. Radiology 266(1):151–158. doi:10.1148/radiol.12112452
18. Zissen MH, Wang ZJ, Yee J, et al. (2013) Contrast-enhanced CT quantification of the hepatic fractional extracellular space: correlation with diffuse liver disease severity. AJR Am J Roentgenol 201(6):1204–1210. doi:10.2214/AJR.12.10039
19. Bandula S, Punwani S, Rosenberg WM, et al. (2015) Equilibrium contrast-enhanced CT imaging to evaluate hepatic fibrosis: initial validation by comparison with histopathologic sampling. Radiology 275(1):136–143. doi:10.1148/radiol.14141435
20. Yoon JH, Lee JM, Klotz E, et al. (2015) Estimation of hepatic extracellular volume fraction using multiphasic liver computed tomography for hepatic fibrosis grading. Invest Radiol 50(4):290–296. doi:10.1097/RLI.0000000000000123
21. Flett AS, Hayward MP, Ashworth MT, et al. (2010) Equilibrium contrast cardiovascular magnetic resonance for the measurement of diffuse myocardial fibrosis: preliminary validation in humans. Circulation 122(2):138–144. doi:10.1161/CIRCULATIONAHA.109.930636
22. Kellman P, Wilson JR, Xue H, Ugander M, Arai AE (2012) Extracellular volume fraction mapping in the myocardium, part 1: evaluation of an automated method. J Cardiovasc Magn Reson 14:63. doi:10.1186/1532-429X-14-63
23. Bandula S, Banypersad SM, Sado D, et al. (2013) Measurement of Tissue interstitial volume in healthy patients and those with amyloidosis with equilibrium contrast-enhanced MR imaging. Radiology 268(3):858–864. doi:10.1148/radiol.13121889
24. Aime S, Caravan P (2009) Biodistribution of gadolinium-based contrast agents, including gadolinium deposition. J Magn Reson Imaging 30(6):1259–1267. doi:10.1002/jmri.21969
25. Landis JR, Koch GG (1977) The measurement of observer agreement for categorical data. Biometrics 33(1):159–174
26. Cademartiri F, Mollet NR, van der Lugt A, et al. (2005) Intravenous contrast material administration at helical 16-detector row CT coronary angiography: effect of iodine concentration on vascular attenuation. Radiology 236(2):661–665. doi:10.1148/radiol.2362040468
27. Materne R, Smith AM, Peeters F, et al. (2002) Assessment of hepatic perfusion parameters with dynamic MRI. Magn Reson Med 47(1):135–142
28. Martini C, Maffei E, Palumbo A, et al. (2010) Impact of contrast material volume on quantitative assessment of reperfused acute myocardial infarction using delayed-enhancement 64-slice CT: experience in a porcine model. La Radiologia medica 115(1):22–35. doi:10.1007/s11547-009-0481-8
29. Van Beers BE, Leconte I, Materne R, et al. (2001) Hepatic perfusion parameters in chronic liver disease: dynamic CT measurements correlated with disease severity. AJR Am J Roentgenol 176(3):667–673. doi:10.2214/ajr.176.3.1760667
30. Klein C, Schmal TR, Nekolla SG, et al. (2007) Mechanism of late gadolinium enhancement in patients with acute myocardial infarction. J Cardiovasc Magn Reson 9(4):653–658. doi:10.1080/10976640601105614
31. Aguirre DA, Behling CA, Alpert E, Hassanein TI, Sirlin CB (2006) Liver fibrosis: noninvasive diagnosis with double contrast material-enhanced MR imaging. Radiology 239(2):425–437. doi:10.1148/radiol.2392050505
32. Martin DR, Lauenstein T, Kalb B, et al. (2012) Liver MRI and histological correlates in chronic liver disease on multiphase gadolinium-enhanced 3D gradient echo imaging. J Magn Reson Imaging 36(2):422–429. doi:10.1002/jmri.23668